Int J Adv Manuf Technol (2013) 67:2717–2726
DOI 10.1007/s00170-012-4686-y

ORIGINAL ARTICLE

# Process and material behavior modeling for a new design of micro-additive fused deposition

**Mario D. Monzón · Ian Gibson · Antonio N. Benítez · Luis Lorenzo · Pedro M. Hernández · María D. Marrero**

Received: 7 April 2012 / Accepted: 17 December 2012 / Published online: 6 January 2013


**Abstract** The aim of this paper is to explore the limits and special requirements for additive manufacturing using polymer extrusion with a nozzle diameter much smaller than the conventional one: 0.050 mm diameter. This work is focused on the nozzle design and analyzes the effect of such a reduced diameter on the extrusion process and on the cooling of material while being deposited on the part. The approach is based on experimental and theoretical studies starting from conventional fused deposition modeling technology where the study tested swelling and cooling of filament material during deposition. Experimental work was used to assess the validity of the theoretical model and the first normal stress equation which estimated a swelling factor (diameter) of 1.249 at 0.087 g/h mass rate. The convection coefficient ($h$) on the plastic part was estimated as$7\,W/m^2K$ on the first deposited layer; considerably lower than some references show.

**Keywords** Melted extrusion modeling · Microfabrication · Fused deposition modeling

M. D. Monzón (✉) · L. Lorenzo · P. M. Hernández · M. D. Marrero
Mechanical Engineering Department, Campus de Tafira Baja, University of Las Palmas de Gran Canaria, Edificio de Fabricación Integrada, Las Palmas de Gran Canaria 35017, Spain
e-mail: mmonzon@dim.ulpgc.es

I. Gibson
Engineering Design and Innovation Centre, National University of Singapore, 9 Engineering Drive 1, Singapore 117576, Singapore

A. N. Benítez
Processing Engineering Department, Campus de Tafira Baja, University of Las Palmas de Gran Canaria, Edificio de Ingenierías, Las Palmas de Gran Canaria 35017, Spain

## 1 Introduction

As commented by Brosseau et al. [1], manufacturing industry has witnessed a rapid increase in demand for micro-production and microcomponents, with electronics and biomedical industries as particularly important markets for this kind of product. Additive manufacturing (AM) [2–4] technologies enable fabrication of end-use products using a layer-by-layer approach with most commercial systems limited in terms of speed of build, build material properties, and overall part accuracy. Attempts have been made to address part accuracy with microstereolithography (μSLA) techniques [5–8]. While successfully creating freeform geometries with high resolution, these parts are somewhat limited to relatively weak and brittle polymer materials. Selective laser sintering of materials has been demonstrated for parts with a resolution of less than 30 μ that promise better material properties [9]. This process is however very complex and expensive. In this research, micro-additive fused deposition (MAFD) is proposed with improved resolution over the existing fused deposition modeling (FDM) process and superior material properties to μSLA at an acceptable cost.

In FDM, parts are fabricated, layer by layer, by extruding a plastic filament onto a platform. In conventional FDM, the smallest available nozzle inner diameter is 0.254 mm which limits the resolution of the fabricated part. Nozzles with diameters below 0.05 mm would allow important steps toward micromanufacturing by this approach. Giannatsis and Dedonisis [10] comment that FDM is very appropriate for direct scaffold fabrication for tissue engineering due to the "flexibility" in material choice. For example, both hydroxyl-apatite or poly-e-caprolactone are suitable to be deposited by FDM. In this context, MAFD could enhance control over scaffold porosity and enable functional gradient structures by reducing the filament dimensions.

The MAFD process faces two particular problems:

- Extrusion of thermoplastic material through a small diameter nozzle exhibits difficulties in terms of high shear stress and shear rate, swelling, pressure drop, and the corresponding feeding of molten material.
- The thin filament, once extruded, has rapid cooling compared with conventional FDM filaments, which could obstruct the nozzle outlet and prevent the bonding of filaments during deposition.

This paper explores the limits of extruding molten thermoplastic material through a nozzle with inner diameter 0.05 mm and corresponding layer thickness of deposited material 0.03 mm. MAFD equipment is still under construction and therefore the experimental starting point is a conventional commercial FDM machine(FDM 8000 from Stratasys) with acrylonitrile butadiene styrene (ABS) P400 (Stratasys) material. These experiments allow us to verify and extrapolate the numerical computations that influence the design of the MAFD system. The design methodology is based on theory of a standard extrusion die and filament cooling model but applied to the micron scale of the proposed MAFD. One important aspect of FDM design is that the extrusion head must be compact and portable to permit three-axis movement for AM. Complex techniques for gradient melting and pressure build-up are difficult to implement under this constraint. It is important therefore to have a comprehensive and accurate predictive model to ensure that the process parameters are under control. This paper therefore addresses the key aspects of nozzle design and material flow behavior through this nozzle.

## 2 Experimental work

Experiments were carried out on a Stratasys FDM 8000 using the recommended commercial ABS, a T16 tip (0.46 mm outlet diameter) and flow rate of 4.95 $mm^3/s$. This experiment tests the behavior of the FDM process under conventional conditions in order to extrapolate relevant conclusions to support the proposed MAFD design, in particular:

- To provide information about normal stress and swelling
- To model the filament cooling and estimate the convective coefficient ($h$)

### 2.1 Determination of swelling diameter factor, $S_w$

Swelling diameter factor ($Sw$) is the final filament diameter divided by the nozzle diameter. Swelling is a well-known phenomenon in extrusion of polymers mainly due to the storage and dissipation of elastic deformation energy, where reversible deformations are partially recovered once the polymer exits the die.

Two factors were varied; envelope temperature (values of 30, 50, and 70 °C) and melt temperature (values of 240, 250, 260, and 270 °C). Fifteen filaments for each combination (total number of observations therefore being 180) were extruded and the diameter was measured by digital micrometer with results shown in Fig. 1.

In order to study the significance of each factor on the swelling, a multifactorial analysis of variance (ANOVA) was implemented (Table 1). This ANOVA table decomposes the variability of diameter in terms of the contributions due to various factors. The $P$ values test the statistical significance of each of the factors. Since two $P$ values are less than 0.05, these factors have a statistically significant effect on diameter at the 95 % confidence level.

Table 2 shows the variance components analysis. The goal of such an analysis is to estimate the amount of variability contributed by each of the factors, called the variance components. In this case, the factor contributing the most variance is melt temperature. Its contribution represents 88.94 % of the total variation in diameter. The mean experimental diameter swelling factor under standard conditions, melt temperature of 270 °C, and envelope temperature of 70 °C as recommended by Stratasys, was found to be 1.169.

### 2.2 Experimental temperature profile of deposited material

This experiment studied the cooling of material during deposition on the FDM machine platform. This is a key issue for modeling the deposition process and enables us to predict how the MAFD system will behave. Nine rectangular samples of 30×20 mm and four layers thick were tested. Two thermocouples (type K, ±1.5 °C) placed on the axis of the rectangle were separated 20 mm from each other. The deposition pattern was 45° related to the $x$-axis. The layer cycle time was around 30 s. Only the bottom layer is in direct contact with the thermocouples as seen in Fig. 2 showing a progressive decrease of peak temperature when the nozzle passes over the thermocouple.

The low measuring speed of the data logger means that the maximum temperature shown in the curve is likely to be lower than the real one. This measurement delay problem was solved using an average regression curve which allows for the heating–cooling trend of deposited material during the process. These regression curves (expressed by an exponential equation) were calculated from the tested samples and are represented in Fig. 3. The curves provide information about the glass transition temperature limit (96 °C) and sintering temperature limit (200 °C) during the deposition process. The experimental temperature profile was the base for determining the real $h$ which predicts the cooling of the filament for the proposed MAFD design.

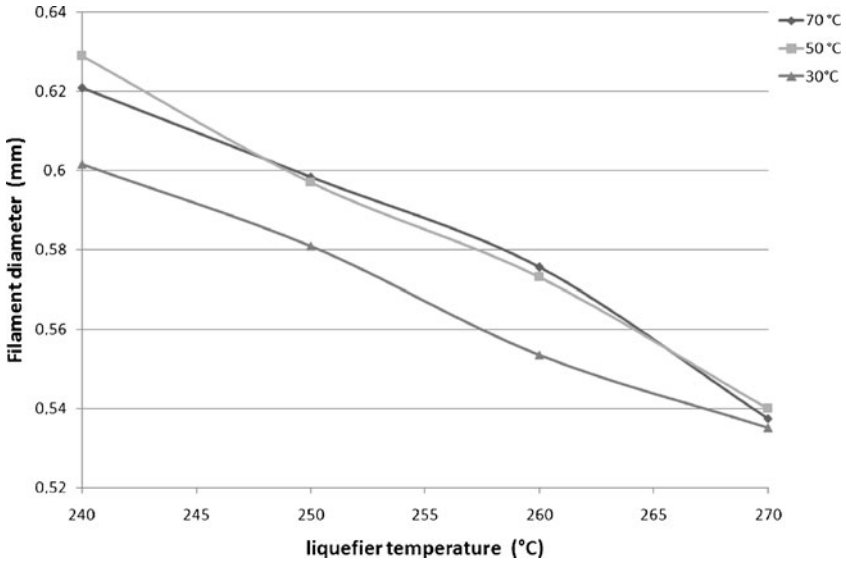


**Fig. 1** Swelling experiment

## 3 Nozzle design and flow modeling

The methodology for designing the geometry of nozzle is typically used in extrusion die design [11] where the main parameters to be controlled are: shear stress, shear rate, residence time, and pressure drop. The nozzle design is mainly focused on the flow channel geometry rather than on constructive characteristics. The relaxation length is a constant section at the end of the flow channel where the polymer deformation is relaxed and therefore swelling takes place. This relaxation length needs to be limited because of two factors:

- Pressure drop in such a thin diameter would greatly increase if the relaxation zone were extended.
- In order to machine the nozzle by electrodischarge machining and taking into account the capability of existing micro-electro-discharge machining technology, the maximum ratio between length and diameter should be 15.

Figure 4 shows the geometry of nozzle-tip with 13 mm total length and 0.75 mm relaxation zone.

Rheological parameters were calculated using two softwares: Dieplast™ and EFD-Lab 8.1. Dieplast™ was developed for designing extrusion dies under non isothermal conditions and is based on fundamental equations (continuity, momentum, and energy) simplified by boundary conditions and specific characteristics of polymer extrusion [11, 12] and solved by finite differences method. Once these simplifications are applied, the equations are as follows:

Simplified momentum equation

$$\frac{\partial P}{\partial X} = -\frac{\partial \tau_{yx}}{\partial Y} \tag{1}$$

Shear stress

$$\tau_{yx} = \mu \times \frac{dV_x}{dY} \tag{2}$$

Simplified energy equation

$$\rho \times C_p \times V_x \times \frac{\partial T}{\partial X} = \lambda \times \frac{\partial^2 T}{\partial Y^2} + \mu \times \left(\frac{\partial V_x}{\partial Y}\right)^2 \tag{3}$$

Where:

| | |
|---|---|
| $P$ | pressure |
| $\tau_{yx}$ | Shear stress |
| $\mu$ | Viscosity |
| Vx | Velocity |
| $T$ | temperature |
| $\rho$ | Density |
| $C_p$ | Specific heat capacity |
| $\lambda$ | thermal conductivity |

**Table 1** Analysis of variance for filament diameter

| Source | Sum of squares | *df* | Mean square | *F* ratio | *P* value |
|---|---|---|---|---|---|
| Main effects | | | | | |
| Envelope temperature | 0.00954888 | 2 | 0.00477444 | 31.29 | 0.0000 |
| Melt temperature | 0.147459 | 3 | 0.0491531 | 322.13 | 0.0000 |
| Residual | 0.0265504 | 174 | 0.000152589 | | |
| Total (corrected) | 0.183559 | 179 | | | |

**Table 2** Variance components analysis

| Source | Sum of squares | *df* | Mean square | Var. comp. | Percent |
|---|---|---|---|---|---|
| Total (corrected) | 0.183559 | 179 | | | |
| Envelope temperature | 0.00954888 | 2 | 0.00477444 | 0.0 | 0.00 |
| Melt temperature | 0.150863 | 9 | 0.0167625 | 0.00110832 | 88.94 |
| Error | 0.0231468 | 168 | 0.000137779 | 0.000137779 | 11.06 |

EFD Lab 8.1 software enables flow simulation and equation of energy considerations as well as thermal conductivity through liquids, solids, and gasses. Since EFD Lab is based on solving time-dependent Navier–Stokes equations, problems are solved through a steady-state approach.

The nozzle was designed using an iterative approach where parameters such as residence time, maximum shear stress and rate, pressure drop, and swelling were kept under control. The ABS P400 material selected for this study was previously characterized by a rheometer (Gottfert 1500) with viscosity curves at different temperatures shown in Fig. 5.

The viscosity model used in Dieplast™ was the Carreau model [11] where the reference temperature was 260 °C. To maintain flow, direct heating of the micronozzle is applied which provides a high temperature at the exit. The relaxation zone is critically defined within the extrusion process with the maximum pressure drop and shear stress. The adjusted equation of Carreau model with William, Landel and Ferry correction (WLF) [13] is as follows:

$$\mu(\dot{\gamma}, T) = \frac{a_t(T) \times A}{\left(1 + a_t(T) \times B \times \dot{\gamma}\right)^C} \tag{4}$$

$$\log a_t = \frac{C_1 \times (T_0 - T_s)}{C_2 + (T_0 - T_s)} - \frac{C_1 \times (T - T_s)}{C_2 + (T - T_s)} \tag{5}$$

Where:

$\mu$ Viscosity (Pa×s)
$\gamma$ Shear rate ($s^{-1}$)
$T$ Temperature (°C)
$A$ 293.924 Pa×s
$B$ 0.008 s
$C$ 0.578
$T_s$ $T_g$+50 °C
$T_g$ Glass transition temperature, 94 °C (ABS P400)
$T_0$ 260 °C (reference temperature for viscosity curve)
$C_1$ −8.86
$C_2$ 101.6

WLF is acceptable when the variation of temperature is within ±30 °C.

Starting from the experimental curves, the implemented viscosity model in EFD Lab 8.1 was the cross-WLF model [11]:

$$\mu = \frac{D_1 \times e^{\left(-\frac{A_1 \times (T - T_g)}{A_2 + T - T_g}\right)}}{1 + \left(\frac{D_1 \times e^{\left(-\frac{A_1 \times (T - T_g)}{A_2 + T - T_g}\right)} \times \dot{\gamma}}{\tau_0}\right)^{1-n}} \tag{6}$$

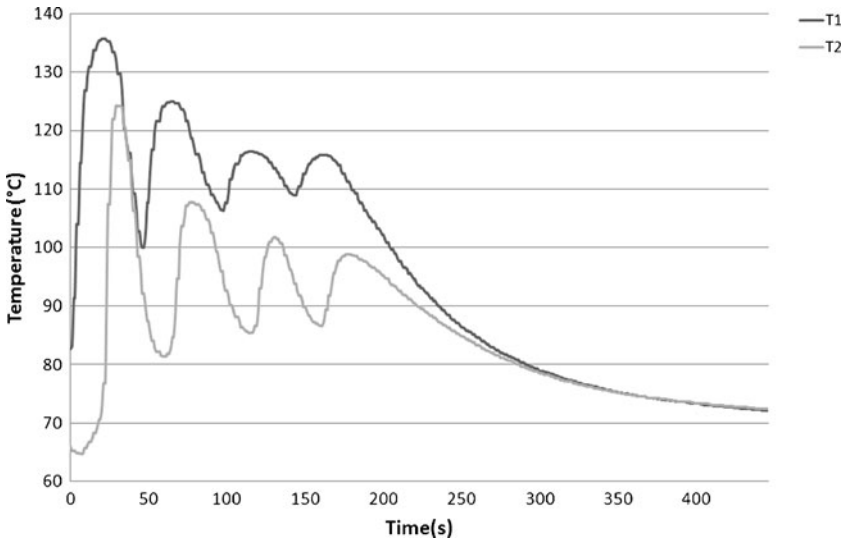


**Fig. 2** Example of temperature profile measured by two thermocouples ($T_1$, $T_2$)

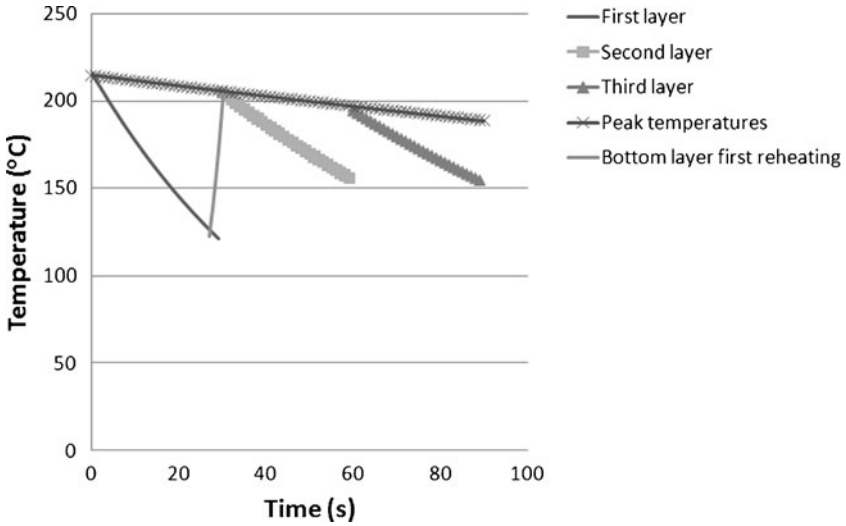


**Fig. 3** Regression temperature profile obtained from average values of measured temperatures

Where:

$\mu$ Viscosity (Pa×s)
$\gamma$ Shear rate ($s^{-1}$)
$T$ Temperature (°K)
$n$ 0.286
$\tau_0$ $1.065\times10^5$ Pa
$D_1$ $9.635\times10^7$ Pa×s
$T_g$ Glass transition temperature, 367.17 °K (ABS P400)
$A_1$ 16.895
$A_2$ 51.6 K

The conditions and parameters considered for simulation were the following:

- ABS PS-400 material (based on Stratasys data sheets)
- Density (in kilograms per cubic meter): 1,050
- Specific heat (joules per kilogram Kelvin): 2,080
- Thermal conductivity (Watts per meter Kelvin): 0.177
- Initial temperature of melt: 266 °C
- Glass transition temperature: 94 °C
- Convective transference heat coefficient with envelope 100 W ($m^2$K) [12, 13]
- Envelope temperature: 70 °C
- Outlet nozzle diameter: 0.05 mm
- Inlet nozzle diameter: 0.5 mm

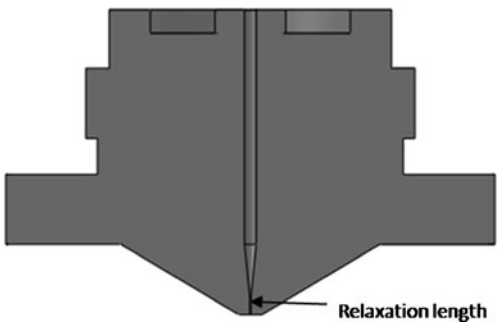


**Fig. 4** Micronozzle geometry, 0.05 mm outlet diameter

- Volume flow: 0.023 $mm^3$/s.
- Outlet filament linear speed: 10 mm/s
- External wall temperature: 270 °C (upper side)

The volume flow of the designed MAFD nozzle is 215 times lower than the conventional FDM nozzle used in experiment (tip 16, on the Stratasys, FDM 8000), and an extrusion rate 2.54 times lower. This low production rate should not be a problem for microfabrication because of the small part size required. For instance, it would take about 12 h to fabricate a 1 $cm^3$ solid piece. Volume flow is limited by rheological parameters due to the small section of channel flow as will be shown later.

One important design feature of the micronozzle is the need for direct heating of the external wall (at least the upper side as seen in Fig. 6). The thin filament is therefore strongly cooled after flowing from the nozzle, which is considered to be a negative issue from the deposition point of view. Thermal and experimental analysis show significant temperature decrease into the nozzle, mainly due to convective flow of heat towards the external envelope. The need to balance this flow explains the additional supply of heat on the external wall of the micronozzle.

The maximum shear stress and shear rate are located in the relaxation zone at the nozzle exit. Shear stress analysis showed 0.166 MPa which is 40 % lower than the reference limit value for ABS at 0.28 MPa. With this value, it is likely that a sharkskin effect may become evident (in the most common polymers this defect occurs over 0.14 MPa) [11]. It is not clear as to the importance this effect may have on overall quality since the polymer will be quickly deposited onto the substrate material and the finish of the filament may not have that strong an influence on the final part. In any case, this issue will be tested by further experiments. Table 3 shows the summary of results obtained by Dieplast™.

As mentioned earlier, the material cools towards the end of the micronozzle because it is only heated on the upper side of the outer wall. Convective losses can be observed in the

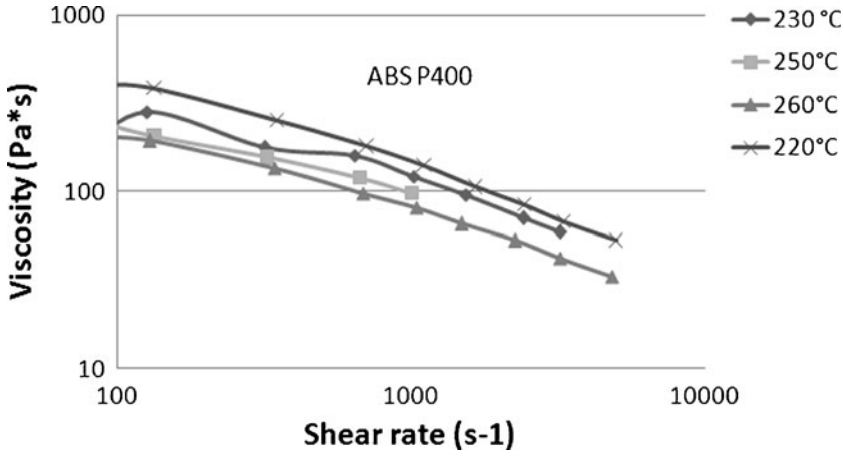


**Fig. 5** Experimental results—viscosity as function of shear rate

cooling curve (Fig. 7). The average temperature at the end of the nozzle is 246 °C (i.e., the flow temperature is decreased by around 20 °C). A similar study for conventional FDM showed the final temperature to be 215 °C, starting from the same initial temperature (266 °C). This significant difference is due to the direct heating of micronozzle. In a verification experiment, the measured temperature by thermocouple, in conventional FDM, of the polymer at the outlet was found to be slightly lower (205 °C) than the calculated one.

## 4 Prediction of MAFD swelling

The prediction of $S_w$ under MAFD process was based on experimental swelling measurement of conventional FDM as previously described. As to the origin of die-swell for viscoelastic fluids, there have been different interpretations such as the effects of normal stress, elastic deformation, orientation, memory, etc. From the macroscopic viewpoint of polymer rheology, the shear or elongation of macromolecules will result in the anisotropy of mechanical properties, producing normal stress difference ($N_1$). In general, the die-swell of polymers is attributable to the initial normal stress. Several authors have proposed expressions for descriptions between $N_1$ and $S_w$. In this research, the model applied is that of Liang [14, 15]

$$N_1 = \tau_w \times \left(S_w{}^4 - 1\right)^{0.5} \tag{7}$$

$$S_w = \left(1 + S_r{}^2\right)^{0.5} \tag{8}$$

$$S_r = \frac{N_1}{\tau_w} \tag{9}$$

For fluids of which the flow obeys the power law, there is an exponential expression of $\tau_w$ (shear stress at the die wall) and $N_1$ [16]

$$N_1 = A \times \tau_w{}^B \tag{10}$$

Where $A$ and $B$ are constants related to the material properties. These were determined by testing the $S_w$ in conventional FDM as seen in Fig. 1. Taking into account the shrinkage of filament, the diameters of samples were corrected with a shrinkage factor (0.006). The methodology for calculating $A$ and $B$ was as follows:

- Average diameter swelling factor determination from experimental measurements at four melt temperatures (240, 250, 260, and 266 °C).
- Calculation of theoretical $\tau_w$ by Dieplast$^{TM}$ (18.7 g/h, 4.95 mm$^3$/s, Stratasys tip with 0.46 mm outlet diameter)
- Determination of experimental $N_1$ introducing $\tau_w$ and experimental $S_w$ in Expression 7

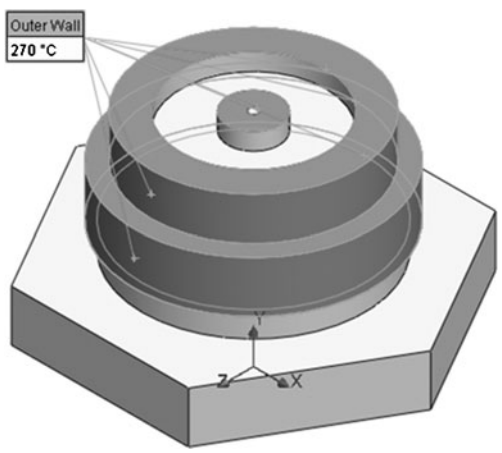


**Fig. 6** Direct heating of upper side of outer wall (270 °C)

**Table 3** Results with Dieplast$^{TM}$

| Maximum shear stress (MPa) | Maximum shear rate ($s^{-1}$) | Residence time (s) | Pressure drop (MPa) |
|---|---|---|---|
| 0.166 | 2,511.3 | 91.2 | 11.9 |

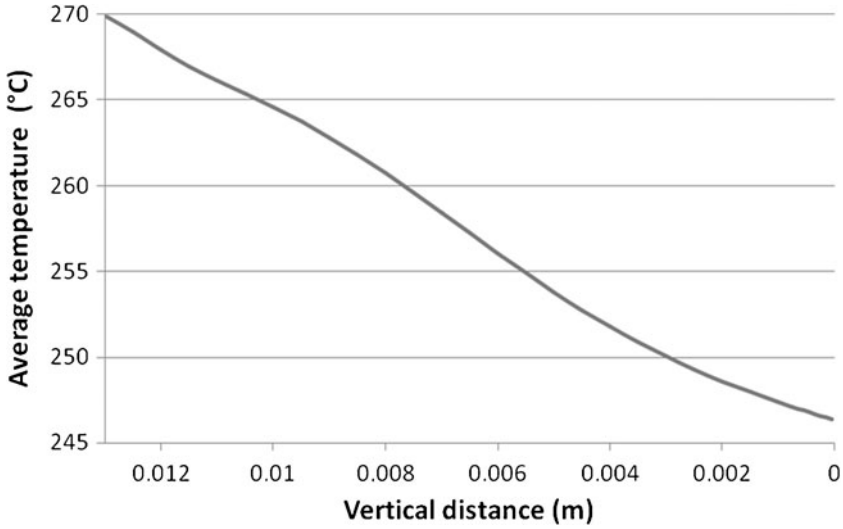


**Fig. 7** Cooling of plastic into the micronozzle channel flow

- With obtained values of $N_1$ and $\tau_w$ adjustment of Eq. 10 for minimum error and calculation of $A$ and $B$.

The resultant equation of $N_1$ for ABS P400was (in megapascal):

$$N_1 = 4.505 \times {\tau_w}^{1.738} \tag{11}$$

Figures 8 and 9 show the evolution of experimental results and the power law model estimated by regression.

If design and processing conditions of the MAFD nozzle provides $\tau_w$=0.166 MPa, the value of $N_1$, applying the Expression 11, will equal to 0.199 MPa.

Therefore from Expressions 8 and 9, substituting both values $N_1$ and $\tau_w$, the estimated diameter swelling factor is 1.249. This means that the final diameter of filament under free flow will be 0.06 mm.

## 5 Prediction of MAFD cooling

One major challenge of MAFD will be to achieve effective bond formation between polymer filaments in the face of high speed of cooling. The lumped capacity model (LCM) method [17–20] has been applied to modeling of FDM bond formation in terms of cooling. This method has been implemented in this work for modeling the cooling of MAFD filaments during deposition.

The simplified general energy Eq. (11) is:

$$\rho c_p \left[\frac{\partial T}{\partial t} + \left(\vec{v} \cdot \nabla\right) T\right] = -\nabla \vec{q} - \tau : \nabla \vec{v} + \phi \tag{12}$$

This equation is simplified by the following hypothesis:

- Steady flow
- Unidirectional flow, corresponding to $x$-axis
- Constant speed
- No viscous forces
- No heat sources neither chemical reactions

Equation 12 gives:

$$\rho \cdot c_p \cdot v_x \cdot \frac{\partial T}{\partial x} = \lambda \cdot \left(\frac{\partial^2 T}{\partial x^2} + \frac{\partial^2 T}{\partial y^2}\right) + \frac{h}{h_{eff}} \cdot (T_\infty - T) \tag{13}$$

Where:

$\rho$ density
$c_p$ specific heat coefficient

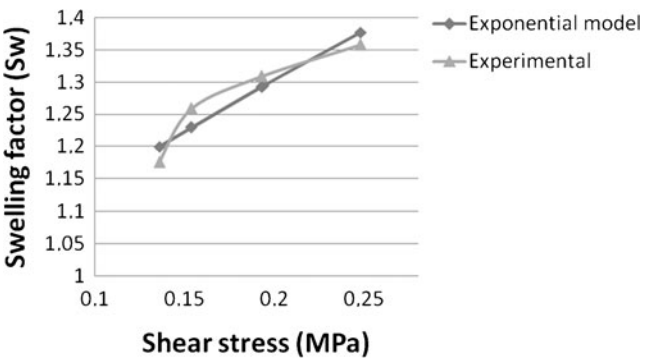


**Fig. 8** Diameter swelling factor. Experimental results and adjusted curve

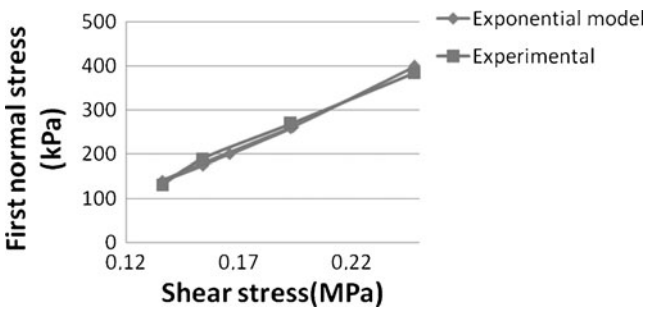


**Fig. 9** First normal stress. Experimental results and adjusted curve

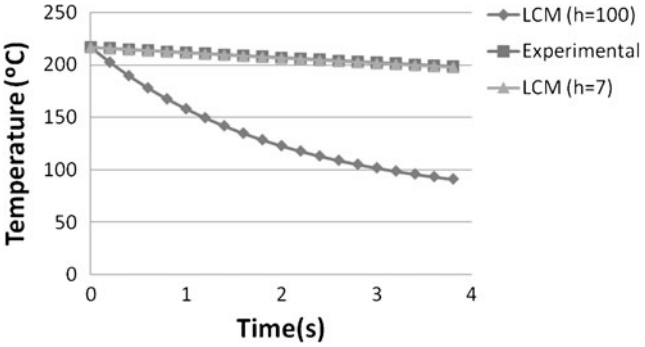


**Fig. 10** Cooling of deposited filament in conventional FDM. Experimental curve (*red*). Lumped capacity model ($h$=100 W/m$^2$K). Adjusted LCM curve at $h$=7 W/m$^2$K

$v_x$ linear speed
$\lambda$ thermal conductivity
$h$ convective coefficient
$h_{\text{eff}}$ $A/P$, $A$ being the cross-section area and $P$ the perimeter of filament
$T_\infty$ temperature of envelope

Since the Biot number remains below 0.1, the cross-sectional conduction heat transfer is considered to be instantaneous assuming a uniform temperature distribution throughout. This conclusion permits removal of the $y$-axis-dependent term and the expression is reduced to the following differential Eq. (4):

$$\rho \cdot c_p \cdot v_x \cdot \frac{\partial T}{\partial x} = \lambda \cdot \frac{\partial^2 T}{\partial x^2} + \frac{h}{h_{eff}} \cdot (T_\infty - T) \tag{14}$$

The analytical solution of Eq. 14 is as follows [4, 20, 21]:

$$T = T_\infty + (T_0 - T_\infty) \cdot e^{-m \cdot x} \tag{15}$$

With

$$m = \frac{(1 + 4 \cdot \alpha \cdot \beta)^{1/2} - 1}{2 \cdot \alpha} \tag{16}$$

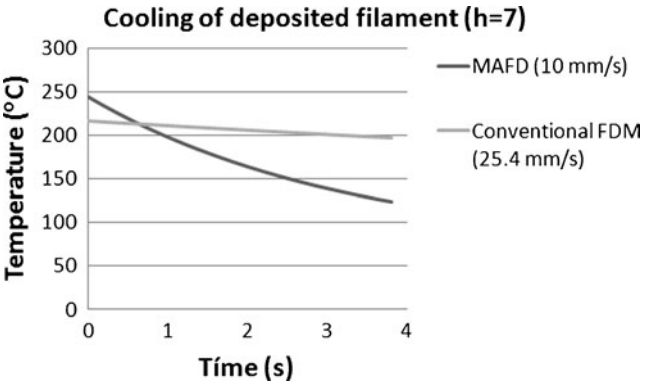


**Fig. 11** Cooling of deposited MAFD filament

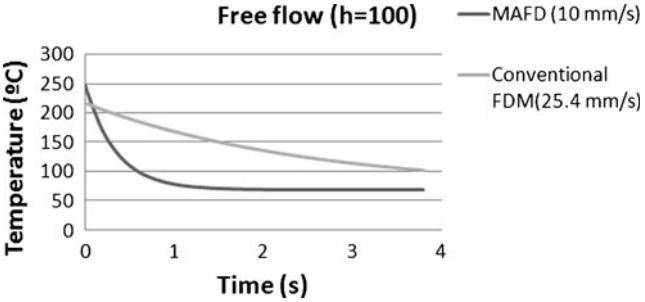


**Fig. 12** Cooling of MAFD filament under vertical free flow

Where

$$\alpha = \frac{\lambda}{\rho \cdot C_p \cdot vx} \tag{17}$$

$$\beta = \frac{h \cdot P}{\rho \cdot C_p \cdot A \cdot vx} \tag{18}$$

Once the filament is deposited, it is assumed the cross section is an ellipse where the perimeter ($P$) and area ($A$) are:

$$P = \pi \times (a + b) \times \left( \frac{64 - 3 \times \varphi^4}{64 - 16 \times \varphi^2} \right) \tag{19}$$

$$\varphi = \frac{a - b}{a + b} \tag{20}$$

$$A = \pi \times a \times b \tag{21}$$

The values of $a$ and $b$ for conventional FDM filament (tip 16) were 0.766 and 0.254 mm, respectively. For the proposed MAFD filament, the values were 0.083 and 0.03 mm, respectively. The speed of filament was 25.4 mm/s in conventional FDM and 10 mm/s in MAFD.

There is a certain level of controversy between several authors in terms of $h$ evaluation. Li estimates this coefficient in the FDM process to be approximately 100 W/m$^2$K [17, 18]. Thomas and Rodríguez [21] used $h$=75 W/m$^2$K. Bellehumeur and Sun [19, 20] chose the range of $h$ as 50–100 W/m$^2$K because this large range should cover other transfer effects, such as heat transfer between the foundation and extruded filaments. In fact, this value has strong influence on cooling speed as seen in Fig. 10.

In order to estimate $h$ based on experimental measurement of temperature, the LCM method was adjusted by experimental results. Figure 10 shows the Eq. 15 profile for two values of $h$, 100 and 7 W/m$^2$K where the second value is clearly the more approximated solution to experimental data. The experimental data corresponds to the average temperature profiles of the first layer (Fig. 7). Evolution of $h$ at the second and third layer could

not be determined because the thermocouples only measured the first layer. The first layer is characterized by the contact of plastic with the foundation or substrate material (usually a foam material) and the following layers are bonded to other previously deposited filaments; therefore, $h$ should be different for the first layer compared with the other upper layers. The lower calculated value of $h$=7 W/m$^2$K, in the preliminary layer, could explain the lower speed of cooling in this layer which assists the bonding of subsequent layers. This hypothesis is confirmed by the micrographs of the cross-sectional area made by Sun et al. [20, 22] where greater neck growth occurs during the first layers. Neck is described as the common surface between adjacent filaments being essential for bonding formation and thus good mechanical properties.

Once $h$ for first layer was estimated, the same methodology was implemented for MAFD. It is clear there is a big difference in terms of cooling speed of conventional FDM and MAFD (Fig. 11). This explains the need to increase the outlet temperature of the polymer compared to conventional FDM. As commented before, the nozzle decreases the polymer temperature due to thermal losses at the end of the channel. In this research, direct heating of the nozzle was introduced and it explains the bigger starting temperature of MAFD curve (247 °C) related to conventional FDM (217 °C). Otherwise, the high pressure drop in MAFD nozzle introduces the need of increasing the final temperature which considerably reduces the pressure drop in such a thin diameter. The temperature of MAFD filament remains above 100 °C (higher than the glass transition temperature for PS 400) at least in a range of 40 mm, which is sufficient for small parts in the field of micromanufacturing. The MAFD-deposited filament reaches a similar temperature to conventional FDM filament at 6-mm length.

If a gap of 0.03 mm between nozzle outlet and foundation is adopted (equivalent to layer thickness), the cooling process could be modeled as a vertical free flow of filament where the free convection from the extruded filament to the envelope air prevails over other effects. In this case, the section of filament is considered as a circle (0.05 mm diameter). However as shown in Fig. 12, the decrease of temperature in such a small gap (0.003 s) is around 1.5 °C; not so significant despite the high speed of cooling. $h$ is considered to have a maximum value of 100 W/m$^2$K according to several authors [17–20]. Further, this small decrease does not introduce the problem of a hypothetical plugging of the nozzle outlet.

## 6 Conclusions

Design and analysis of a new tip for micro-additive fused deposition (outlet diameter, 0.05 mm) started from experimental analysis of a conventional FDM tip in a Stratasys FDM 8000. Maximum value of shear stress (0.166 MPa), shear rate (2,511 s$^{-1}$), and residence time (91.2 s) remained below limits for ABS in the proposed MAFD nozzle simulation. Pressure drop into flow channel of 11.9 MPa was helped by an increase of temperature due to direct heating of the nozzle tip which represents a novelty compared to conventional tips. Experimental results of swelling allowed calculation of the coefficients of the first normal stress power law equation ($A$=4.505, $B$=1.738). The first normal stress equation and Liang expression provided 1.249 as the predicted diameter swelling factor in the proposed MAFD system. Temperature profiles of deposited filament in experimental analysis of conventional FDM were the base for calculating by regression an approximated value of 7 W/m$^2$K as convective transmission coefficient in the first layer. The direct heating of the tip also allows higher temperature of deposited material, balancing the high speed of cooling of the MAFD filament. The volume flow of MAFD nozzle is 215 times lower than the conventional FDM nozzle one (tip 16), with a filament speed 2.54 times lower. This low production rate should not be a problem however in terms of microfabrication because of small part size likely to be required in this field.

The future works will include experimental equipment for testing the new MAFD nozzle. The relatively high pressure drop into the micronozzle channel obstructs the commercial options of feeding a filament by rollers. Also, feeding by small screw extruders are limited to reflow of material due to high pressure at the die inlet. The apparently more suitable option would be a high precision linear electrical actuator. Otherwise, new materials for MAFD should be developed providing better behavior in terms of fluidity and viscoelastic properties under such a thin channel flow.

## References


1. Brousseau EB, Dimov SS, Pham DT (2010) Some recent advances in multi-material micro- and nano-manufacturing. Int J Adv Manuf Technol 47:161–180
2. Chua CK, Leong KF, Lim CS (2003) Rapid prototyping: principles and applications. World Scientific, Singapore
3. Levy GN, Schindel R, Kruth J (2003) Rapid manufacturing and rapid tooling with layer manufacturing (LM) technologies, state of the art and future perspectives. CIRP Anals Manuf Tech 52:589–586
4. Gibson I, Rosen DW, Stucker B (2010) Additive manufacturing technologies. Springer, New York
5. Yang H, Tsiklos G, Ronaldo R, Ratchev S (2010) Application of microstereolithography technology in micromanufacturing. Micro Ass Tech Appl 260:171–176
6. Lee IH, Woo Cho D (2003) Micro-stereolithography photopolymer solidification patterns for various laser beam exposure conditions. Int J Adv Manuf Tech 22:410–416
7. Choi JW, Wicker R, Lee SH, Choi KH, Ha CS, Chung I (2009) Fabrication of 3D biocompatible/biodegradable micro-scaffolds using dynamic mask projection microstereolithography. J Mater Process Tech 209:5494–5503
8. Lee SJ, Kang HW, Park JK, Rhie JW, Hahn SK, Cho DW (2007) Application of microstereolithography in the development of

three-dimensional cartilage regeneration scaffolds. Biomed Microdevices 10:233–241
9. Regenfuss P, Streek A, Hartwig L, Klötzer S, Brabant T, Horn M, Ebert R, Exner H (2007) Principles of laser micro sintering. Rapid Prototyping J13:204–212
10. Giannatsis J, Dedoussis V (2009) Additive fabrication technologies applied to medicine and health care: a review. Int J Adv Manuf Technol 40:116–127
11. Michaeli W (1992) Extrusion dies for plastics and rubber. Hanser, Germany
12. Monzón MD, Collar E, Castany FJ (1998) Aplicación C.A.E. para el diseño de cabezales de extrusión de termoplásticos y elastómeros. Revista de PlásticosModernos 505:79–87
13. Williams ML et al (1955) The temperature dependence of relaxation mechanism in amorphous polymers and other glass-forming liquids. J Am Chem Soc 7:3701–3706
14. Liang JZ (2002) Predictions of normal stress difference during circular duct flow of polymer melts. Polym Test 21:619–622
15. Liang JZ (1996) Prediction of primary normal stress difference from extrudateswell of rubber compound. Plast Rub Compos Pro 25:257–259
16. Carreau PJ, Choplin L, Clermont JR (1985) Exit pressure in capillary die data. Polymer Eng Sci 25:669–676
17. Li L, Gu P, Sun Q, Bellehumeur C (2003) Modeling of bond formation in FDM process. Transact NAMRI/SME 31:613–620
18. Li L, Sun Q, Bellehumeur GP (2002) Composite modeling and analysis for fabrication of FDM prototypes with locally controlled properties. J Manuf Process 4:129–132
19. Bellehumeur C, Li L, Sun Q, Gu P (2003) Modeling of bond formation between polymer filaments in the fused deposition modeling process. J Manuf Process 6:170–178
20. Sun Q, RizviGM BCT, Gu P (2008) Effect of processing conditions on the bonding quality of FDM polymer filaments. Rapid Prototyping J 14:72–80
21. Thomas JP, Rodríguez JF (2000) Modeling the fracture strenght between fused deposition extruded roads. Solid Freeform Fabrication Symposium Proceeding, Austin, TX, USA
22. Rodríguez J, Thomas JP, Renaud JE (2000) Characterization of mesostructure of fused deposition acrylonitrile-butadiene-styrene materials. Rapid Prototyping J 6:175–185